Supporting Information:

PySHS : A Python Open Source Software For Second Harmonic Scattering

*Lotfi Boudjema, Hanna Aarrass, Marwa Assaf, Marie Morille, Gaelle Martin-Gassin, Pierre-Marie Gassin**

ICGM, ENSCM, CNRS, Univ Montpellier, 34296 Montpellier Cedex 5, France

1°) Full expression of the coefficients a_{Π}^{Θ}, b_{Π}^{Θ}, c_{Π}^{Θ}

The coefficient a_{Π}^{Θ}, b_{Π}^{Θ}, c_{Π}^{Θ} where Π =V or H and Θ = 90° or 180° are defined by:

$$I_{SHS}{}^{\Theta}(\gamma,\Pi) = a_{\Pi}^{\Theta}.cos^4(\gamma) + b_{\Pi}^{\Theta}.\, cos^2(\gamma)sin^2(\gamma) + c_{\Pi}^{\Theta}.sin^4(\gamma) \quad \text{(S1)}$$

The full derivation of equations (3-9) in the manuscript into the equation S1 gives:

$$a_{\mathrm{V}}^{90} = a_{\mathrm{V}}^{180} = \langle \beta_{t,XXX}\beta_{t,XXX}^{*} \rangle \quad \text{(S2)}$$

$$c_{\mathrm{V}}^{90} = c_{\mathrm{V}}^{180} = \langle \beta_{t,XYY}\beta_{t,XYY}^{*} \rangle \quad \text{(S3)}$$

$$b_{\mathrm{v}}^{90} = b_{\mathrm{v}}^{180} = \langle 4\beta_{t,XXY}\beta_{t,XXY}^{*} + \beta_{t,XXX}\beta_{t,XYY}^{*} + \beta_{t,XXX}^{*}\beta_{t,XYY} \rangle \quad \text{(S4)}$$

$$a_{\mathrm{H}}^{90} = \langle \beta_{t,ZXX}\beta_{t,ZXX}^{*} \rangle \quad \text{(S5)}$$

$$a_{\mathrm{H}}^{180} = \langle \beta_{t,YXX}\beta_{t,YXX}^{*} \rangle \quad \text{(S6)}$$

$$c_{\mathrm{H}}^{90} = \langle \beta_{t,ZYY}\beta_{t,ZYY}^{*} \rangle \quad \text{(S7)}$$

$$c_{\mathrm{H}}^{180} = \langle \beta_{t,YYY} \beta_{t,YYY}^{*} \rangle \quad \text{(S8)}$$

$$b_{\mathrm{H}}^{90} = \langle 4\beta_{t,ZXY} \beta_{t,ZXY}^{*} + \beta_{t,ZXX} \beta_{t,ZYY}^{*} + \beta_{t,ZXX}^{*} \beta_{t,ZYY} \rangle \quad \text{(S9)}$$

$$b_{\mathrm{H}}^{180} = \langle 4\beta_{t,YXY} \beta_{t,YXY}^{*} + \beta_{t,YXX} \beta_{t,YYY}^{*} + \beta_{t,YXX}^{*} \beta_{t,YYY} \rangle \quad \text{(S10)}$$

2°) Comparison of the PySHS computation VS other softwares

2.1) Comparison *PySHS* VS *HRS_Computing*[1]

The configuration of the dipole in simulation Figure 3a) and 3b) of the manuscript are given as input parameter of the *HRS_Computing* software. The *HRS_Computing* output is presented in Figure S1.

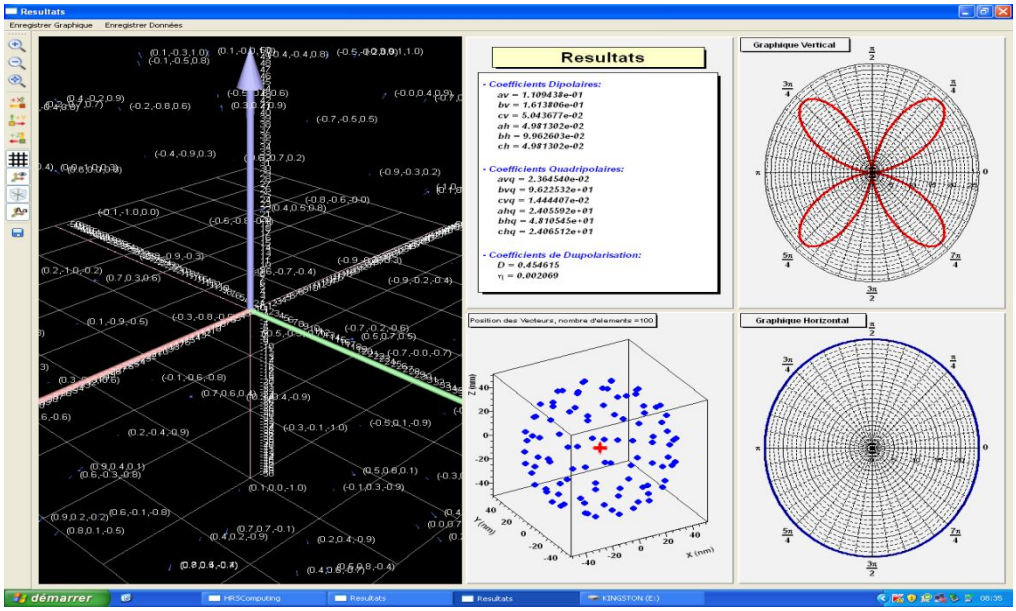

Figure S1. Output of the HRS_Computing software.

To use the same notation as defined in the manuscript, the coefficients av,bv,cv,avq,bvq,cvq have been converted into I_2 and I_4 coefficient. It gives:

$I_2^{90,\mathrm{V}} =$ 0.00; $I_4^{90,\mathrm{V}} =$ -0.99 ; $I_2^{90,\mathrm{H}} =$ 0.00 ; $I_4^{90,\mathrm{H}} =$ 0.00

This *HRS_Computing* output gives the same results as the *SHSlinear* program of the PySHS package. (see Figure 4a in the manuscript).

2.2) Comparison PySHS versus NLS_Simulate[2]

Figure S2 presents the comparison of the SHS angular pattern computed for different radius spheres with the *SPHERE_angle* program of the PySHS package and with the *NLS_Simulate* software.

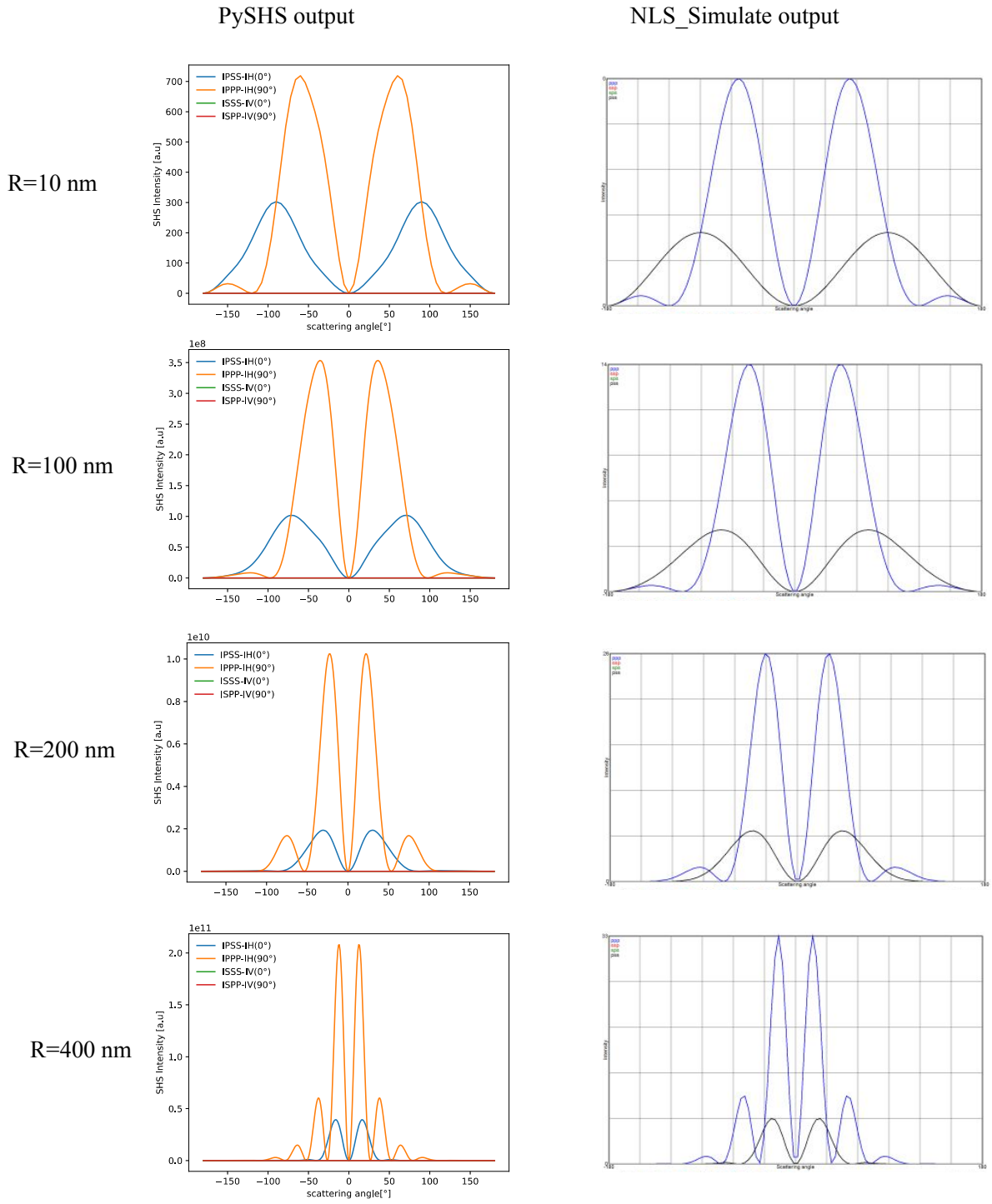

Figure S2. Comparison of the PySHS output (on the left) and NLS_Simulate output (on the right) for spheres of respectively radius equal to 10, 100, 200 and 400 nm. The input parameters are: refractive index n=1.33, Incident wavelength=800 nm, and surface second order tensor, $\chi^{(2)}_{zzz}$=1 all the other components equal to 0.

2.3) Capabilities table

	HRS Computing	NLS Simulate	PySHS
Polarization resolved SHS calculation	X	NO	X
Angular distribution SHS calculation	NO	X	X
Calculation for all shape system	X	NO	X
Calculation for all size system	NO	X	X
Operating System: Windows	X	X	X
Operating System: MacOS	NO	NO	X

3°) Differents simulation of PySHS

Figure S3 presents the polarization plot generated with the SHS program for different disorder of the assembly described by σ.

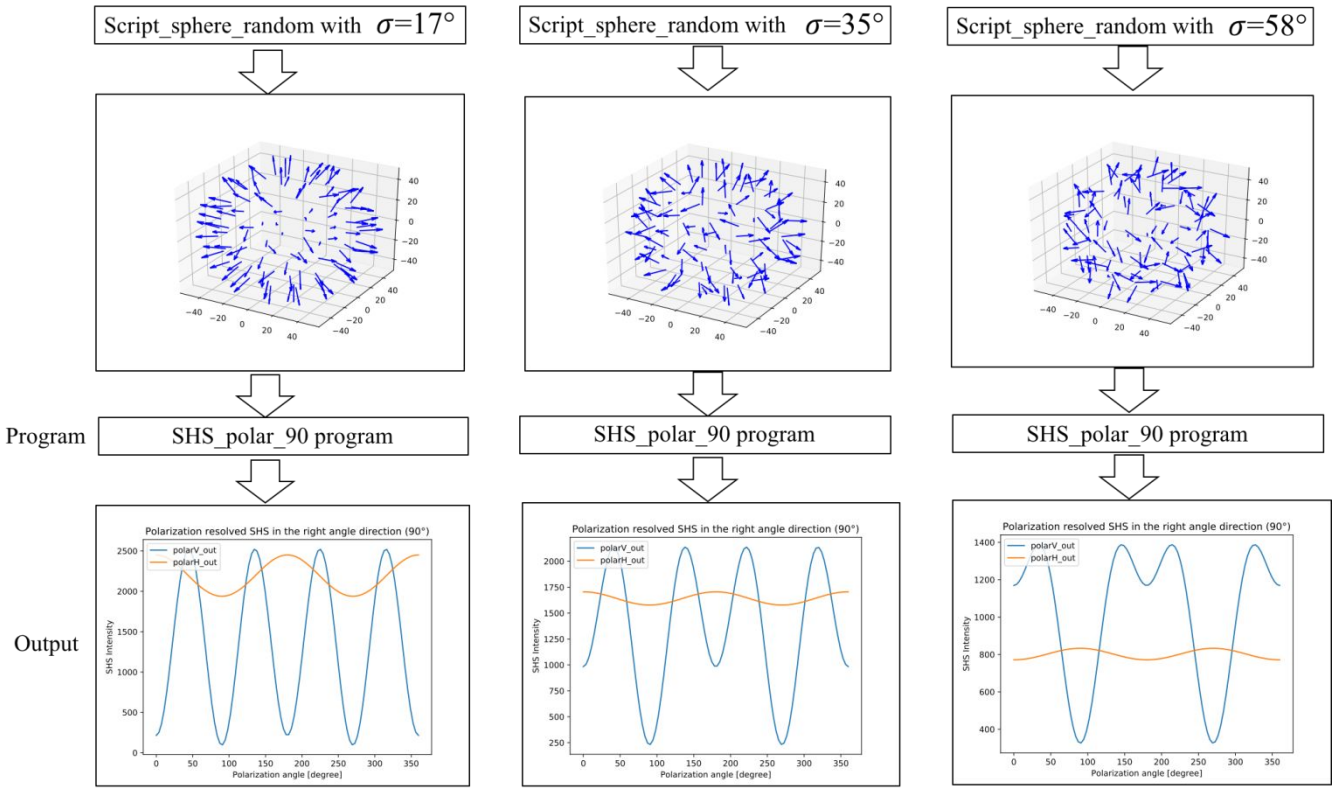

Output

$I_4^{90,V} = -0.884$
$I_2^{90,V} = 0.044$
$I_2^{90,H} = 0.117$
$I_4^{90,H} = 0.002$

$I_2^{90,V} = 0.277$
$I_4^{90,V} = -0.553$
$I_2^{90,H} = 0.039$
$I_4^{90,H} = -0.000$

$I_2^{90,V} = 0.410$
$I_4^{90,V} = -0.272$
$I_2^{90,H} = -0.038$
$I_4^{90,H} = 0.000$

Figure S3. Computational polarization plot obtained with different molecular assembly disorders: a) σ=17°, b) σ=35° and c) σ=58°. The other input parameters are the same as in Figure 3 of the manuscript.

Figure S4 show how the global arrangement from spherical geometry to spheroid geometry characterized with its two radius a and c change the polarization plot. In this study, the dipoles are radially oriented as in Figure S3 simulations.

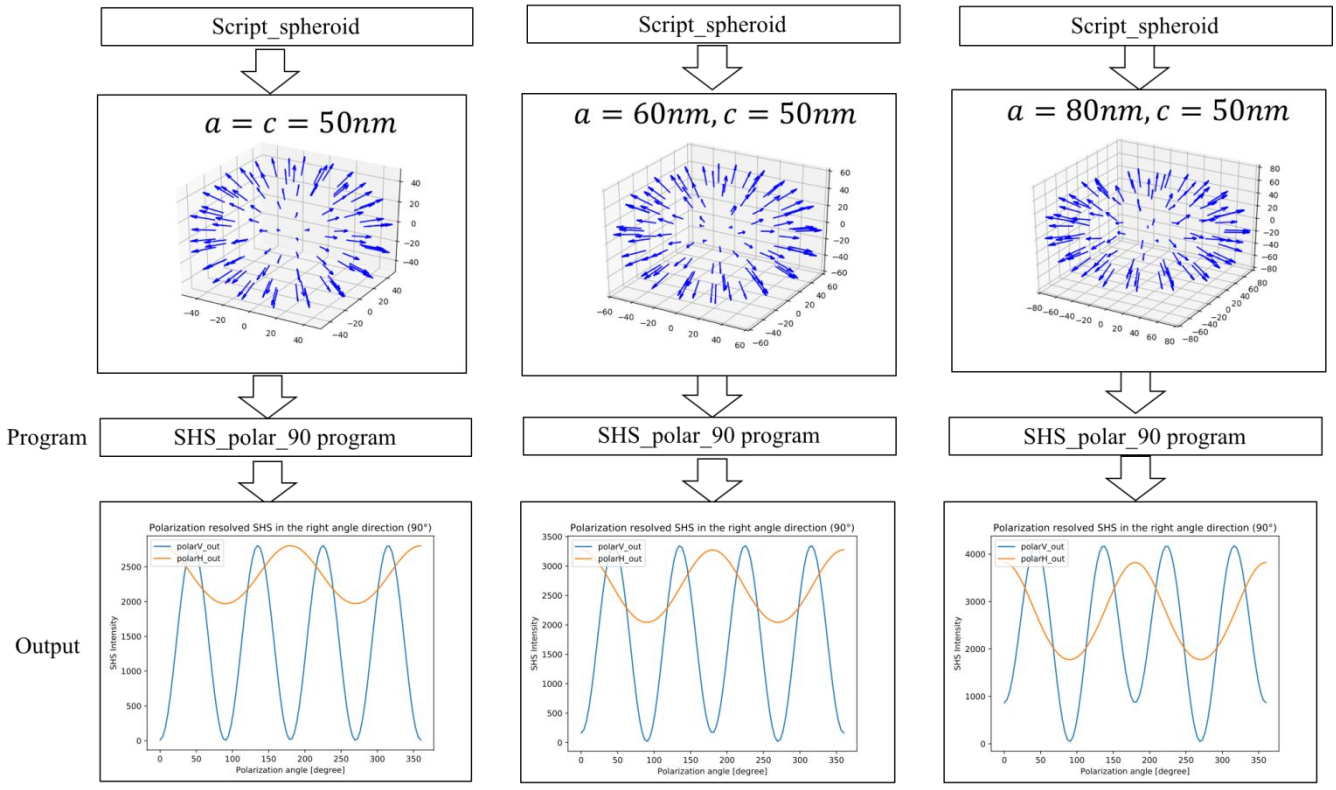

Figure S4. Computational polarization plot obtained with different molecular assemblies: a) spherical assembly, b) spheroid assembly with radius equal to 60 and 50 nm. c) spheroid assembly with radius equal to 80 and 50 nm. The other input parameters are the same as in Figure S3.

4°) Sample preparation

4.1°) Preparation of the liposomes

Liposomes were synthesized by lipid film hydratation rehydratation methods (Bangham method[3]). Briefly, 1,2-dioleoyl-sn-glycero-3-phospho-(1'-rac-glycerol) (DOPG) phospholipid were dissolved in chloroform at a concentration of 5 mg/mL. 2.4 mL are introduced in a 25 mL flask and vapored in a rotary vacuum evaporator. The formed lipid film was hydrated overnight at 4°C with PBS to a final concentration of 3mg/mL. The suspension was then extruded with a nitrogen extrudate apparatus mounted with 100 nm polycarbonate membranes.

4.2°) Characterization of the liposomes

The size of the liposome was characterized with Dynamic Light Scattering (DLS) using NanoZS (Malvern Instrument, UK), see Figure S5. The characteristic size of the liposome is 110 nm +/- 10 nm with PDI= 0.08, see below the size distribution obtained with DLS. is around 110 nm.

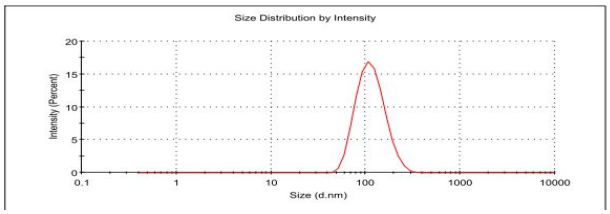

Figure S5. Characterization of the liposomes using DLS

4.3°) Preparation of the dye inclusion

$5.0x10^{10}$ liposomes in PBS are mixed with 5µM of the organic dye DIA4 and the solution is incubated at 55°C during one hour.

References:

1. Carrazza, S.; Duboisset, J. https://sourceforge.net/projects/hrscomputing/ (2013).
2. De Beer, A. G. F; Roke, S. https://www.epfl.ch/labs/lbp/page-89617-en-html/ (2010).
3. Bangham, A. D.; Standish, M. M.; Watkins, J. C., Diffusion of Univalent Ions across the Lamellae of Swollen Phospholipids. *J. Mol. Biol.* **1965**, *13*, 238-IN27.